Biomedicine & Pharmacotherapy 107 (2018) 475–483

Contents lists available at ScienceDirect

Biomedicine & Pharmacotherapy

journal homepage: www.elsevier.com/locate/biopha

Identification of *N*-Hydroxycinnamamide analogues and their bio-evaluation against breast cancer cell lines

Akhilesh Kumar Shukla[a], Hamidullah[b,c,d], Manoj Kumar Shrivash[a], Vishwa Deepak Tripathi[e], Rituraj Konwar[c,d], Jyoti Pandey[a,*]

[a] Department of Chemistry, Babasaheb Bhimrao Ambedkar University (A Central University), Lucknow 226025, UP, India
[b] Department of Dermatology, University of Wisconsin Madison, WI 53706, USA
[c] Endocrinology Division, CSIR-Central Drug Research Institute (CDRI), Sector 10, Jankipuram Extension, Sitapur Road, Lucknow 226031, India
[d] Academy of Scientific and Innovative Research (AcSIR), CSIR-Central Drug Research Institute Campus, Lucknow 226031, India
[e] Department of Chemistry, Maharani Kalyani College Laheriasarai, Lalit Narayan Mithila University, Darbhanga 846001, Bihar, India

ARTICLE INFO

Keywords:
Breast cancer
MDA-MB-231
MCF-7
N-Hydroxycinnamamide
HEK-293

ABSTRACT

The present study demonstrates the identification of *N*-hydroxycinnamamide derivatives and their anticancer potential against human triple-negative breast cancer cell line MDA-MB-231, MCF-7 and non-malignant origin cell line, HEK-293 (human embryonic kidney). MTT assay was studied with HEK-293 cell line. Anticancer potential of the *N*-hydroxycinnamamide derivatives were compared with marked drug Tamoxifen through in vitro study. The compound numbers **3b** and **3h** exhibit most potent activity against antagonistic breast cancer cells (MDA-MB-231) with IC_{50} **13μM** and **5μM** respectively. **Compound 3h** promotes DNA fragmentation and induction of apoptosis. Furthermore, loss of mitochondrial membrane potential induced by **compound 3h**. The major mechanism of **compound 3h** for anti-breast cancer activity was probably initiation of reactive oxygen species (ROS) in cancer cells thereby persuading apoptotic cell deaths in cancer cells.

1. Introduction

Cancer is one of the most severe public health issue around the globe according to the World Health Organization (WHO) [1]. Among various type of cancers breast cancer is also one of the major causes of cancer death among women worldwide. Due to its complex cancer biology, it is necessary to use multiple therapeutic modalities. So far, the conventional treatments for breast cancer are surgical intervention, hormonal therapy, radiotherapy and chemotherapy. It is merely responsible for 20–25% of all cancer cases and 15–18% of cancer deaths among women [2]. Although the emergence of drugs such as Tamoxifen and Toremifene makes chemotherapy a viable choice for breast cancer patients, the development of drug resistance and severe side effects are unresolved problems in clinical oncology [3]. Therefore, the search for novel anti-cancer compounds with improved features is needed. In recent oncology research, different breast cancer cell lines have been applied by investigators for drug discovery purposes and among these cells estrogen non-dependant MDA-MB-231 is one of the most extensively used model [4].

Hydroxamic acids or hydroxamates are carboxylic acids or aldehyde analogues where −COOH group or −CHO group has been replaced by −CONHOH or −CONHR [5]. Hydroxamic acids are well known as efficacious molecules in the field of cancer chemotherapy and as a mutagenic agent. Several hydroxamates based drugs are functioning very good in clinics for cancer chemotherapy such as SAHA [6,7], PXD-101 (Belinostat,Topotarget) [8] and LBH-589 (panobinostat) [9], which are approved by the U.S. Food and Drug Administration (FDA) in October 2006, July 2014 and February 2015, respectively (Fig. 1). There are some other hydroxamate based molecules are in clinical trials, such as m-carboxycinnamic acid bishydroximic acid (CBHA) [10], SB-939 (phase II) [11] and 4SC-201 (Resminostat, phase II) [12].

Among various derivatives of hydroxamic acid, SAHA (Suberoylanilide Hydroxamic Acid) is considered as a potent anticancer agent [13]. These molecules possess very good chelating ability [14]. This chelating property makes them very favourable for enzyme inhibition and therefore hydroxamates possess a special place in cancer drug discovery research. Due to these special properties hydroxamates are very interesting group for scientists from all over the world. Several research groups have synthesized different hydroxamic acid moieties with well-known inhibitors of matrix metalloproteinases (MMPs) [15], peptidyldeformylases [16], adenylyl cyclases (ACs) [17], inosine monophosphate dehydrogenase (IMPDH), histone deacetylase (HDAC)

* Corresponding author.
E-mail address: drjyotibbau@gmail.com (J. Pandey).

https://doi.org/10.1016/j.biopha.2018.08.015
Received 11 June 2018; Received in revised form 24 July 2018; Accepted 6 August 2018

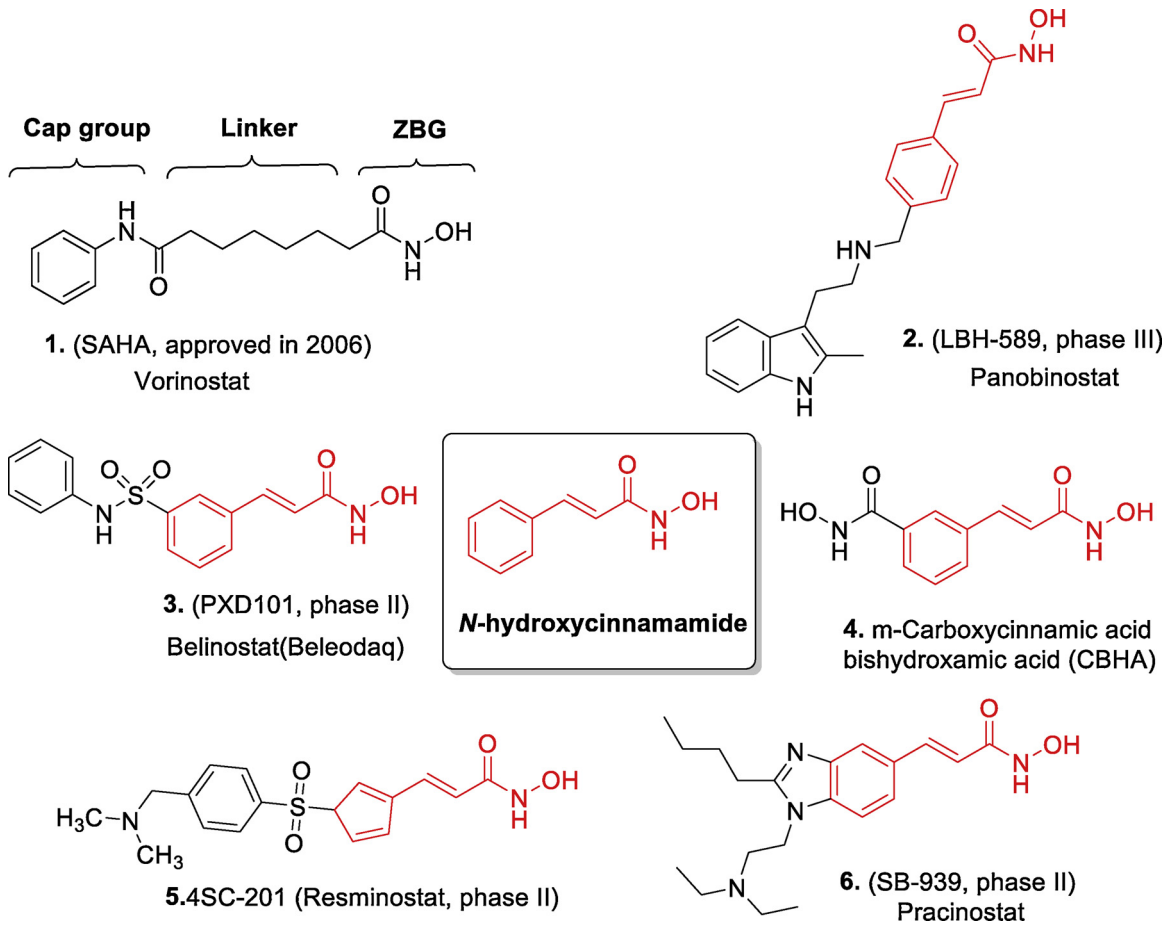

Fig. 1. Approved and clinical HDACLs with *N*-hydroxycinnamamide fragment highlighted in red.

[15], carbonic anhydrase [18], tumor necrosis factor converting enzyme (TACE, ADAM17) [19] and TNF-α–converting enzyme [20]. One research group reported antileukemic activity in hydroxamic acids [21,22]. Azaindolehydroxamic acid derivatives are known to possess potent anti-HIV activities [23] while sulfonamidohydroxamates are good anti-osteoarthritis agents [24–26]. In addition to these interesting properties this moiety is also present in many growth factors [27], food additives [28], antibiotics [29,30], antitumors [31], antifungals [32], cell division factors and enzyme inhibitors [33,34]. They have also shown inhibition against melanogenesis [18]. As many enzymes are inhibited by hydroxamates, several physiological processes are affected by this versatile class. Some molecules with hydroxamic acid functionality have also been reported as NO donors [35] and the acetylated hydroxamates derivatives can act as effective aspirin analogues by prostaglandin H2 synthase inhibition [36,37].

It is evident from literature survey that hydroxamic acid derivatives have attracted scientists for their potential as highly efficacious in combating various etiological factors associated with cancer [38]. They have also been used as acyl cation equivalents for the preparation of carbonyl compounds and *N*-methoxyamides as precursors of *N*-methoxy-*N*-acylnitrenium ions in electrophilic aromatic substitutions and as precursor for β-lactams synthesis [39,40]. Different *N*-benzoxyamides as precursors of hydroxamic acids, are known for different biological activities including anti-inflammatory [41] antiasthmatic [42] antimetastatic [43] antibiotic [44] psychotropic [33] insecticidal [45] acaricidal [46] and nematocidal activity [33]. In this article we present anticancer property of hydroxamic acid derivatives to show that this single functional moiety has not only fit in the receptor site but also create a diversified activity.

Present work demonstrates synthesis of simple hydroxamic acids by aldehyde using HWE reaction and synthesis of 2-*O*-alkyl benzhydroxamic acids.

2. Materials and methods

2.1. Materials

All chemicals, reagents and solvents were purchased from Sigma Aldrich and Merck. Thin layer chromatography was performed using silica gel 60 F254 plates with detecting agent iodine vapours, Merck Silica gel (60–120 mesh) was used for column chromatography. IR spectra were recorded as thin films or in chloroform soln with a Perkin–Elmer Spectrum RX-1 (4000–450 cm^{-1}) spectrophotometer. 1H and 13C NMR spectra were recorded on a Brucker DRX-400 and 101 MHz in DMSO-d6. Chemical shift values are reported in ppm relative to SiMe4 as internal reference, unless otherwise stated; s (singlet), d (doublet), t (triplet), m(multiplet); J in hertz. FAB mass spectra were performed using a mass spectrometer Jeol SX-102 and ESI mass spectra with Quattro II (Micromass). Melting points were obtained manually by capillary methods and are uncorrected. Elemental analyses were performed on a Perkin–Elmer 2400 II elemental analyzer. The organic extracts were dried over anhydrous Na2SO4 and evaporation of the solvent was carried out on a rotary evaporator under reduced pressure.

2.2. Synthesis of α, β-unsaturated hydroxamic acids

The starting acrylate derivatives (**2a-k**) were prepared by the Horner-Wadsworth-Emmons (HWE) olefination of different aromatic aldehydes (**1a-k**) with triethylphosphonoacetate in the presence of LiOH in THF at ambient temperature. The reaction of acrylate

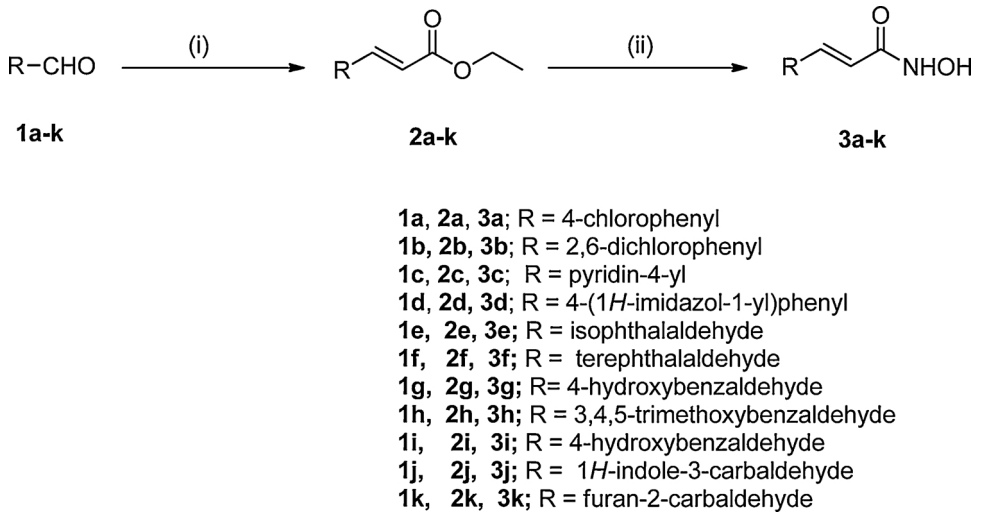

Scheme 1. Synthesis of *N*-Hydroxycinnamamide derivatives, Reagents and conditions.
(i) LiOH (1.1eq), TEPA (1.1eq), THF, RT (ii) $NH_2OH.HCl$ (5 eq), KOH (10 eq), CH_3OH, 0 °C- RT.

derivatives (2a-k) with hydroxylamine hydrochloride in the presence of KOH in methanol at 0–5 °C results in the formation of respective *N*-hydroxyacrylamide (**3a-k**) in moderate to excellent yields with 99.8% purity. (Scheme 1).

2.3. Synthesis of 2-O-alkyl benzhydroxamic acids

Compounds methyl 2,4-dihydroxybenzoate (**4**) on chemoselective benzylation with benzyl bromide in acetone in the presence of anhydrous K_2CO_3 and catalytic amount of tetrabutylammonium bromide (TBAB) affords methyl 4-(benzyloxy)-2-hydroxybenzoate (**5**) in good yield. Latter (**5**) on allylation with allyl bromide in refluxing THF in the presence of anhydrous K_2CO_3 and a catalytic amount of tetrabutylammonium bromide (TBAB) resulted in methyl 2-(allyloxy)-4-(benzyloxy)benzoate (**6**) [47]. Finally, the methyl benzoate derivative (**6**) on reaction with hydroxylamine hydrochloride in the presence of solid KOH in methanol at 0–5 °C led to the formation of desired 2-alloxy-4-benzyloxy *N*-hydroxybenzamide derivative (**7**) in 85% yield (Scheme 2).

2.4. General synthesis of hydroxamic acid

To the stirring mixture of desired acrylate (1 mmol) in methanol added with hydroxylamine hydrochloride (5 mmol) and KOH (10 mmol) at 0–5 °C, it was stirred at room temperature until consumption of the starting material (according to TLC). After the completion of reaction, the solvent was evaporated under reduced pressure to give a crude mass, which was purified by column (SiO_2, 60–120 mesh) using a gradient of EtOAc /hexane as eluent to give the pure compounds **3a-k, 7** in excellent yields.

(E)-3-(4-chlorophenyl)-N-hydroxyacrylamide (3a)

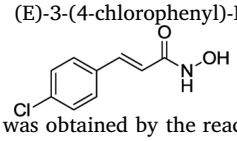

It was obtained by the reaction of ethyl-3-(4-chlorophenyl)acrylate **2a** (0.5 g, 2.37 mmol), hydroxyl amine hydrochloride (0.824 g, 11.8 mmol) and KOH (1.32 g, 23.7 mmol) in methanol at 0–5 °C to room temperature to gave the corresponding acrylamide **3a** in 84% yield (0.85 g) as a white solid, mp 140–142 °C; IR(ν_{max},cm^{-1}): 3416, 3039, 1650, 1090, 754, ^{1}H NMR (400 MHz, DMSO-d_6); δ_H 9.57–9.31 (1H, brs, NH) 7.60–7.58 (2H, d, J = 8.3 Hz, Ar-H), 7.46-7.44 (2H, d, J = 8.3 Hz, Ar-H), 7.41 (1H, brs, CH), 6.49–6.45 (1H, m, J = 15.8 Hz), 2.08 (1H, s, OH); ^{13}C NMR (101 MHz, DMSO-d_6); δ_C 162.9, 137.5, 134.3, 134.1, 129.6, 129.4, 120.2. HRMS: Calcd. accurate mass for ($C_9H_9ClNO_2$), 197.0316. Found. $[M+H]^+$ 198.0313.

(E)-3-(2, 6-dichlorophenyl)-N-hydroxyacrylamide (3b)

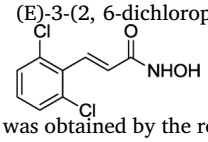

It was obtained by the reaction of ethyl-3-(2,6-dichlorophenyl) acrylate **2b** (0.5 g, 2.03 mmol), hydroxyl amine hydrochloride (0.708 g, 10.15 mmol) and KOH (1.14 g, 20.3 mmol) in methanol at 0–5 °C to room temperature to gave the corresponding acrylamide **3b** in 74% yield (0.85 g) as a white solid, mp 142–144 °C; IR (ν_{max}, cm^{-1}); 3684, 3411, 1602, 1523, 757, ^{1}H NMR (400 MHz, DMSO-d_6); δ_H 10.31–10.05 (1H, brs, NH), 7.54 (2H, m, Ar-H), 7.49–7.45 (1H, d, J = 16.0 Hz) 7.39–7.35 (1H, t, J = 7.8 Hz) 6.55–6.51 (1H, d, J = 15.9 Hz); ^{13}C NMR (101 MHz, DMSO-d_6); δ_C 162.0, 134.1, 132.4, 132.0, 130.8, 129.5, 128.1; HRMS: Calcd. accurate mass for ($C_9H_8Cl_2NO_2$); 230.9927. Found. $[M+H]^+$ 231.9940.

(E)-3-(pyridin-4-yl)-N-hydroxyacrylamide (3c)

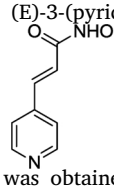

It was obtained by the reaction of ethyl-3-(pyridin-4-yl)acrylate **2c** (0.5 g, 2.82 mmol), hydroxyl amine hydrochloride (0.980 g, 14.1 mmol) and KOH (1.58 g, 28.2 mmol) in methanol at 0–5 °C to room temperature to gave the corresponding acrylamide **3c** in 70% yield (0.77 g) as a yellow solid, mp 156–158 °C; IR (ν_{max}, cm^{-1}); 3435, 2855, 1611, 1512, 1400, 756, 669; ^{1}H NMR (400 MHz, DMSO-d_6); δ_H 10.97 (1H, brs, NH),

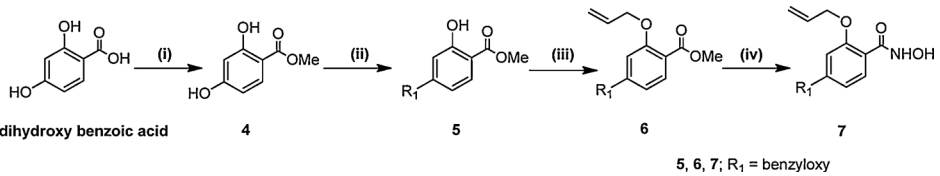

Scheme 2. Synthesis of O-alkyl benzamide derivative.
Reagents and conditions (i) MeOH, 20% H_2SO_4, reflux (ii) Benzyloxybromide, K_2CO_3, Acetone, RT, (iii) Allyl bromide, K_2CO_3, TBAB, THF, reflux (iv) $NH_2OH.HCl$, KOH, MeOH, 0–30 °C.

8.60–8.65 (2H, d, J = 5.9 Hz, Ar-H), 7.53–7.51 (2H, d, J = 6.0 Hz, Ar-H), 7.44–7.40 (1H, d, J = 15.8 Hz), 6.70–6.67 (1H, d, J = 15.8 Hz); ^{13}C NMR (101 MHz, DMSO-d_6); δ_C 161.7, 150.2, 141.9, 135.8, 123.6, 121.5 HRMS: Calcd. accurate mass for ($C_8H_9N_2O_2$), 165.0659. Found. [M + H]$^+$ 166.0672.

(E)-3-(4-(1*H*-imidazol-1-yl) phenyl)-N-hydroxyacrylamide (3d)

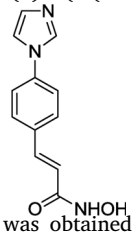

It was obtained by the reaction of (E)-ethyl 3-(4-(1H-imidazol-1-yl) phenyl)acrylate **2d** (1.0 g, 4.12 mmol), hydroxyl amine hydrochloride (1.434 g, 20.63 mmol) KOH (2.31 g, 40.27 mmol) in methanol at 0–5 °C to room temperature to gave the corresponding acrylamide **3d** in 85% yield (0.85 g) as a light brown solid, mp 158–160 °C; IR (ν_{max}, cm^{-1}): 3435, 2855, 1611, 1512, 1400, 756, 669; ^{1}H NMR (400 MHz, DMSO-d_6); δ_H 10.21–9.64(1H, brs, NH), 8.31 (1H, m, Ar-H), 7.78 (1H, m, Ar-H),7.70 (4H, m, Ar-H) 7.50–7.46 (1H, d, J = 15.9 Hz, CH), 7.12 (1H, s, Ar-H), 6.53–6.49 (1H, d, J = 16.0, CH), ^{13}C NMR (101 MHz, DMSO-d_6); δ_C 163.0, 137.7, 137.4, 135.9, 133.8, 130.5, 129.4, 120.8, 120.0, 118.2; HRMS: Calcd. accurate mass for ($C_{12}H_{12}N_3O_2$), 229.0924. Found: [M + H]$^+$ 230.0924

(2E,2E')-3,3'-(1,3-phenylene)bis(N-hydroxyacrylamide) (3e)

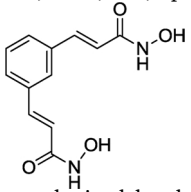

It was obtained by the reaction of diethyl-1,3-(3-phenyl)acrylate **2e** (1.0 g, 3.55 mmol), hydroxyl amine hydrochloride (1.20 g, 18.75 mmol) and KOH (1.92 g, 3.45 mmol) in methanol at 0–5 °C to room temperature to gave the corresponding acrylamide **3e** in 75% yield (0.75 g) as a brown solid, mp 123–125 °C; IR (ν_{max}, cm^{-1}): 3415, 2865, 1655, 1570, 1295, 858, 755, 659; ^{1}H NMR (400 MHz, DMSO-d_6) δ_H 10.04 (2H, brs, NH), 7.84 (1H, s, Ar-H), 7.57-7.55 (2H, d, J = 7.4 Hz, Ar-H), 7.48–7.44 (2H, d, J = 16.0 Hz, CH), 7.42 (1H, s, Ar-H), 6.58–6.54 (2H, d, J = 15.76 Hz, CH), ^{13}C NMR (101 MHz, DMSO-d_6) δ 163.0, 138.0, 135.9, 128.5, 127.3, 120.4, 39.2. HRMS: Calcd. accurate mass for ($C_{12}H_{13}N_2O_4$), 248.0870. Found. [M + H]$^+$ 249.0872.

(2E,2E')-3,3'-(1,4-phenylene)bis(N-hydroxyacrylamide) (3f)

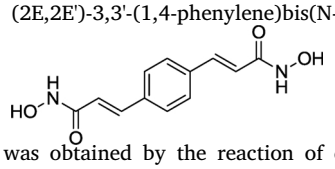

It was obtained by the reaction of diethyl-1,4-(3-phenyl)acrylate **2f** (1.0 g, 3.52 mmol), hydroxyl amine hydrochloride (1.16 g, 17.65 mmol) and KOH (1.87 g, 3.55 mmol) in methanol at 0–5 °C to room temperature to gave the corresponding acrylamide **3f** in 79% yield (0.79 g) as a brown solid, mp 124–126 °C;IR (ν_{max}, cm^{-1}); 3515, 2955, 1661, 1580, 1305, 765, 679; ^{1}H NMR (400 MHz, DMSO-d_6); δ_H 9.92 (2H, brs, NH), 7.66–7.54 (4H, m, Ar-H), 7.43–7.41 (2H, d, J = 10.2 Hz, CH), 6.55–6.52 (2H, d, J = 11.0 Hz, CH), ^{13}C NMR (101 MHz, DMSO-d_6); δ_C 163.0, 138.1, 138.0, 136.2, 134.3, 131.6, 129.5, 128.50, 127.1, 120.2, 39.8. HRMS: Calcd. accurate mass for ($C_{12}H_{13}N_2O_4$), 248.0870. Found. [M + H]$^+$ 249.0867.

(E)-3-(4-(benzyloxyphenyl)-*N*-hydroxyacrylamide (3g)

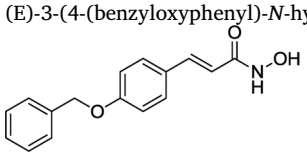

It was obtained by the reaction of (E)-ethyl 3-(4-(benzyloxy)phenyl) acrylate **2g** (1.0 g, 3.35 mmol), hydroxyl amine hydrochloride (1.16 g, 16.75 mmol) and KOH (1.87 g, 3.35 mmol) in methanol at 0–5 °C to room temperature to gave the corresponding acrylamide **3g** in 75% yield (0.75 g) as a brown solid, mp 123–125 °C; IR (ν_{max}, cm^{-1}): 3409, 3104, 1669, 1537, 1491, 1232, 747, 641; ^{1}H NMR (400 MHz, DMSO-d_6); δ_H 10.55 (1H, brs, NH), 7.52–7.50 (2H, d, J = 8.1 Hz, Ar-H), 7.46–7.38 (5H, m, Ar-H) 7.35–7.33 (2H, d, J = 8.0 Hz, Ar-H), 6.41–6.37 (1H, d, J = 16.56 Hz, CH), 6.35–6.32 (1H, d, J = 15.68 Hz, CH), 5.14 (2H, s, OCH_2), ^{13}C NMR (101 MHz, DMSO-d_6); δ_C 159.8, 143.9, 138.4, 137.2, 128.9, 128.3, 128.0, 117,1, 115.6, 69.7; HRMS: Calcd. accurate mass for ($C_{16}H_{16}NO_3$), 269.1125. Found. [M + H]$^+$ 270.1116.

(E)-*N*-hydroxy-3-(3,4,5-trimethoxyphenyl)acrylamide (3h)

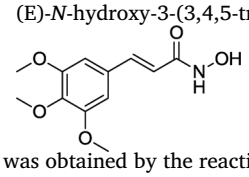

It was obtained by the reaction of (E)-ethyl 3-(3,4,5-trimethoxyphenyl) acrylate **2h** (1.0 g, 3.35 mmol), hydroxyl amine hydrochloride (1.16 g, 16.75 mmol) and KOH (1.87 g, 3.35 mmol) in methanol at 0–5 °C to room temperature to gave the corresponding acrylamide **3 h** in 85% yield (0.85 g) as a brown solid, mp 120–122 °C, IR(ν_{max},cm^{-1}): 3392, 2919, 1673, 1507, 1290, 703; ^{1}H NMR (400 MHz, DMSO-d_6) δ 10.57 (1H, brs, NH) 7.42–7.39 (2H, d, J = 9.56 Hz, Ar-H), 6.99–6.96 (1H, d, J = 15.72 Hz, CH), 6.45–6.41 (1H, d, J = 15.88 Hz, CH), 3.81 (s, 6 H), 3.68 (s, 3 H).^{13}C NMR (101 MHz, DMSO-d_6) δ 153.5, 139.1, 138.9, 130.9, 118.8, 105.4, 60.5, 56.3. HRMS: Calcd. accurate mass for ($C_{12}H_{16}NO_5$), 253.1023. Found: [M + H]$^+$ 254.1032.

(E)-*N*-hydroxy-3-(4-(2-(hydroxyamino)-2-oxoethoxy)phenyl)acrylamide (3i)

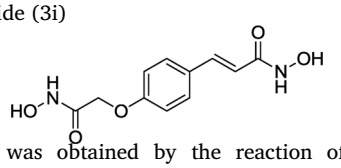

It was obtained by the reaction of (E)-ethyl 3-(4-(2-ethoxy-2-oxoethoxy)phenyl)acrylate **2i** (1.0 g, 3.35 mmol), hydroxyl amine hydrochloride (1.16 g, 16.75 mmol) and KOH (1.87 g, 3.35 mmol) in methanol at 0–5 °C to room temperature to gave the corresponding acrylamide **3i** in 72% yield (0.72 g) as a brown solid, mp 122–124 °C; IR (ν_{max},cm^{-1}): 3402, 3019, 1680, 1290, 767, 658; ^{1}H NMR (400 MHz, DMSO-d_6); δ_H 10.71 (1H, brs, NH), 9.06 (1H, brs, NH) 7.52–7.50 (2H, d, J = 6.64 Hz, Ar-H), 7.43–7.39 (1H, d, J = 15.72 Hz, CH), 6.91 (2H, m, Ar-H), 6.36–6.32 (1H, d, J = 1 Hz, CH), 4.50 (2H, s, OCH_2), ^{13}C NMR (101 MHz, DMSO-d_6); δ_C164.5, 163.5, 159.2, 138.3, 129.4, 128.5, 117.3, 115.5, 66.2, 40.5, 40.3, 40.1, 39.9, 39.7, 39.5, 39.3. HRMS: Calcd. accurate mass for ($C_{13}H_{15}N_2O_5$), 278.0975. Found. [M + H]$^+$ 279.0972.

(E)-*N*-hydroxy-3-(1-methyl-1H-indol-3-yl) acrylamide (3 j)

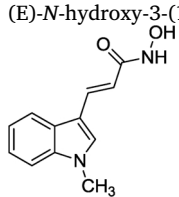

It was obtained by the reaction of (E)-ethyl 3-(1-methyl-1H-indol-3-yl) acrylate **2j** (1.0 g, 3.35 mmol), hydroxyl amine hydrochloride (1.16 g, 16.75 mmol) and KOH (1.87 g, 3.35 mmol) in methanol at 0–5 °C to room temperature to gave the corresponding acrylamide **3j** in 80% yield (0.80 g) as a brown solid, mp 125–127 °C; IR (ν_{max}, cm^{-1}): 3449, 3129, 2830, 1664, 1507, 1215; ^{1}H NMR (400 MHz, DMSO-d_6) δ 11.90 (s, 1H, NH), 7.53–7.51 (2H, d, J = 8.12 Hz, Ar-H), 7.30–7.26 (1H, d, J = 16.2 Hz, CH), 7.23 (1H, s, Ar-H), 7.21–7.19 (2H, d, J = 7.92 Hz, Ar-H), 6.32–6.28 (1H, d, J = 15.92 Hz, CH), 3.82 (3H, s, CH_3).^{13}C NMR (101 MHz, DMSO-d_6) δ 169.0, 138.3, 138.2, 135.2, 125.9, 122.9, 121.5,

120.3, 112.6, 111.1, 40.6, 33.3. HRMS: Calcd. accurate mass for ($C_{12}H_{13}N_2O_2$), 216.0972. Found. $[M+H]^+$ 217.0978

(*E*)-3-(furan-2-yl)-*N*-hydroxyacrylamide (3k)

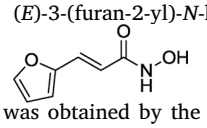

It was obtained by the reaction of (E)-ethyl 3-(furan-2-yl)acrylate **2k** (0.5 g, 2.82 mmol), hydroxyl amine hydrochloride (0.980 g, 14.1 mmol) and KOH (1.58 g, 28.2 mmol) in methanol at 0–5 °C to room temperature to gave the corresponding acrylamide **3k** in 70% yield (0.77 g) as a yellow solid, mp 156–158 °C, IR(ν_{max},cm^{-1}): 3412, 3129, 1683, 1510, 652; ^{1}H NMR (400 MHz, DMSO-d_6) δ 9.86 (1H, brs, NH), 7.75 (s, 1 H), 7.28–7.25 (1H, d, J = 15.6 Hz, CH), 6.75 (s, 1 H), 6.56 (s, 1 H), 6.28–6.24 (1H, d, J = 15.6 Hz, CH),^{13}C NMR (101 MHz, DMSO-d_6) δ 163.0, 151.3, 145.1, 126.1, 116.8, 114.1, 112.8. HRMS: Calcd. accurate mass for ($C_7H_8NO_3$), 153.0499. Found: $[M+H]^+$ 154.0489.

2-(allyloxy)-4-(benzyloxy)-N-hydroxybenzamide (7)

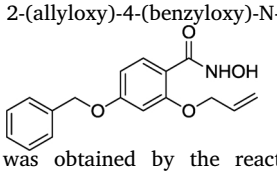

It was obtained by the reaction of methyl-2-allyloxy-4-benzyloxybenzoate **6** (1.0 g, 3.35 mmol), hydroxyl amine hydrochloride (1.16 g, 16.75 mmol) and KOH (1.87 g, 3.35 mmol) in methanol at 0–5 °C to room temperature to gave the corresponding acrylamide **7** in 85% yield (0.85 g) as a brown solid, mp 124–126 °C; IR (ν_{max}, cm^{-1}): 3399, 3019, 1641, 1607, 1491, 1421, 1215, 1182, 757, 669; ^{1}H NMR (400 MHz, DMSO-d_6); δ_H 9.08 (1H, brs, NH), 7.60–7.57 (1H, m, Ar-H) 7.45–7.43 (2H, d, J = 7.1 Hz, Ar-H), 7.41–7.37 (2H, t, J = 7.0 Hz, Ar-H), 7.35–7.31 (1H, m, Ar-H), 6.68–6.67 (2H, m, Ar-H), 6.08-5.99 (1H, m, C*H*=CH_2), 5.41–5.36 (1H, dd, J_1 = 17.2 Hz, J_2 = 1.1 Hz, C*H*=CH_2), 5.28–5.25 (1H, d, J = 10.5 Hz, C*H*=CH_2), 5.13 (2H, s, OCH_2),4.67–4.66 (2H, d, J = 4.9 Hz, OCH_2); ^{13}C NMR (101 MHz, DMSO-d_6); δ_C 163.6, 161.7, 157.3, 137.0, 133.6, 128.9 (2C), 128.4, 128.2 (2C), 118.4, 115.3, 106.9, 100.9, 69.9, 69.3. HRMS: Calcd. accurate mass for ($C_{17}H_{18}NO_4$), 299.1230. Found: $[M+H]^+$ 300.1221.

3. Bioassay

3.1. Cell culture

Breast Cancer cell lines, MDA-MB-231 and MCF-7 were originally obtained from American type of cell culture collection (ATCC), USA and stock was maintained in laboratory. Non-malignant origin cell line, HEK-293 (human embryonic kidney) was obtained from institutional cell repository of animal tissue culture facility. Cells were cultured in CO_2 incubator at 37 °C with 5% CO_2 and 95% humidity in RPMI-1640 growth medium supplemented with 10% FBS and 1% of antibiotic and antimycotic solution.

3.2. Cell viability assay

MTT (3-(4,5-dimethylthiazol-2 yl)-2,5-diphenyl tetrazolium bromide) assay was performed to determine cell viability upon compound exposure as per method described earlier. In brief, cells @ 1×10^4/well were seeded in 96 well microculture plates in 100 µl RPMI-1640 medium and incubated for 24 h at 37 °C in a CO_2 incubator. Compounds were diluted to required concentration in phenol red free RPMI-1640 medium supplemented with 2% FBS. After 24 h of incubation, cells were treated with desired concentration of compounds and respective vehicle alone control for 24 h. At the end of incubation, 10 µL (5 mg/mL) of MTT (Sigma, USA) was added and incubated for another 3 h. Finally, supernatant was carefully discarded and 200 µl of DMSO was added to dissolve formazan crystals under gentle shaking in plate shaker (Biosan, USA) and absorbance at 570 nm wavelength was recorded in a microplate reader (Microquant, BioTek).

3.3. Cell cycle analysis

Effect of **compound 3h** of cell cycle phase distribution was measured with flow cytometry technique using propidium iodide (PI) staining method. For this, 1×10^6 MDA-MB-231 cells were seeded in six well plates and allowed to grow for 24 h. Next day, cells were treated with **compound 3h** for another 24 h. At the end of that incubation peroid, cells were harvested, washed with PBS and fixed with 70% chilled ethanol. Fixed cells were washed with PBS and stained with PI (30 µg/mL) in PBS containing 10 µg/mL RNase A for 30 min at room temperature in dark condition. DNA content of the cells was measured using a FACS Calibur flow cytometer using FACScan (Becton Dickinson) and percentages of cells in each phases of cell cycle were calculated.

3.4. Hoechst staining

To determine effect of **compound 3h** on nuclear morphology, fluorescent microscopy was carried out using Hoechst staining. 1×10^6 MDA-MB-231 cells were seeded in 6-well culture plates for 24 h. After another 24 h of treatment with **compound 3h**, cells were washed with PBS, fixed with 4% paraformaldehyde for 15 min and subsequently cells were permeabilized with 3% paraformaldehyde containing 0.1% tritonX-100 for 10 min. Finally, cells were stained with 1 µg/ml of Hoechst-33358 (Sigma, USA) for 30 min at room temperature, washed with PBS and photographed using fluorescent microscopy.

3.5. Apoptosis assay

Effect of **compound 3h** on cell death was carried out using flow cytometry based Annexin V-FITC/PI apoptosis kit (Sigma, USA). 1×10^6 MDA-MB-231 cells were seeded in 6-well culture plates for 24 h, followed by treatment with **compound 3h** for another 24 h. After 24 h of treatment, cells were harvested, washed with PBS and stained with Annexin V-FITC/PI kit for 10 min. Finally, samples were analyzed by flow cytometry (FACScan, Becton Dickinson).

3.6. Mitochondrial membrane potential analysis

To analyze effect of **compound 3h** on mitochondrial membrane potential, 1×10^6 MDA-MB-231 cells were seeded in 6-well culture plates and grown for 24 h. Grown cell monolayers were treated with **compound 3h** for another 24 h. At the end of treatment, cells were harvested, washed with PBS and incubated with 5 µg of JC-1 dye for 30 min at room temperature, followed by washing and re-suspension in 300 µl PBS. Finally, JC-1 stained MDA-MB-231 cells were analyzed by flow cytometry using FACScan (Becton Dickinson).

3.7. Reactive oxygen species (ROS) analysis

ROS was measured in terms of reactive oxygen induced fluorescence of DCF-DA, basically a non-fluorescent cell staining dye. For this, 1×10^6 MDA-MB-231 cells were seeded in 6-well plates for 24 h, followed by treatment with **compound 3h** for 24 h. At the end of incubation, cells were harvested, washed with PBS and then fixed with chilled absolute methanol. Cells were stained with 10 µg/mL DCFH-DA and incubated at room temperature in dark condition for 30 min. After incubation, cells were centrifuged and re-suspended in 300 µl PBS and analyzed by flow cytometry (FACScan, Becton Dickinson, USA).

3.8. Evaluation of biological activity

All the synthesized compounds were screened for anti-cancer activity in both MCF-7 (ER + ve) and MDA-MB-231 (ER-ve) cells and HEK-293 cells using MTT assay (Table 1).

Table 1
Anti-proliferative effect of synthesized compounds with cell line MCF-7, MDA-MB-231 and HEK-293.

Structure	Code	MCF-7 IC_{50} μM	MDA-MB-231 IC_{50} μM	HEK-293 IC_{50} μM
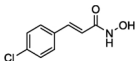	**3a**	> 50	> 50	> 50
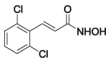	**3b**	30 ± 2.26	13 ± 2.62	> 50
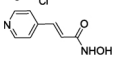	**3c**	> 50	45 ± 1.43	> 50
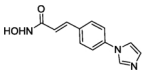	**3d**	> 50	39 ± 3.45	> 50
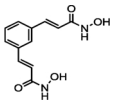	**3e**	> 50	42 ± 2.37	> 50
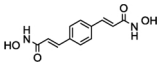	**3f**	> 50	41 ± 3.12	> 50
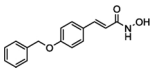	**3 g**	34.3 ± 1.54	35 ± 3.45	> 50
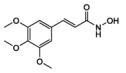	**3 h**	31 ± 3.24	5 ± 2.16	> 50
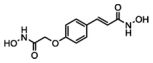	**3i**	> 50	41 ± 2.54	> 50
	**3 j**	> 50	43 ± 3.43	> 50
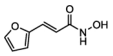	**3k**	42 ± 2.32	> 50	> 50
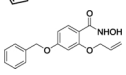	**7**	45 ± 3.34	37 ± 3.12	> 50
	Tamoxifen	10 ± 1.32	15 ± 2.04	50 ± 2.18

3.9. Docking study on EGFR protein target of breast cancer in silico molecular docking analysis

We have analyzed the synthesized compounds through docking study using Autodock 4.2 to exploit the possible interactions between ligands and EGFR kinase. The analysis shows that amino acids (Leu $_{844}$, Lys_{745}, Val_{726}, Met_{793}, and Cys_{775}) in EGFR protein is the potential target site for binding of **compound3b** by formation of hydrogen bond with chloro and hydroxamic acid groups of **compound3b** (Fig. 2). The **compound3e** interacted with amino acids (Leu_{718}, Val_{726} and Ala_{743}), **compound3f** interacted with amino acids (Ala $_{743}$, Val $_{726}$, Leu $_{844}$, Met_{766} and Thr_{854}), **compound3g** interacted with amino acids (Leu_{844}, Leu_{792}, Leu $_{718}$, Ala_{743}, Thr_{854} and Met_{793}), **compound3h** interacted with amino acids (Thr_{854}, Ala_{743}, Leu_{718}, Val_{726} and Leu_{844}) (Table 2), and **compound7** interacted with amino acids (Leu_{792}, Leu_{718}, Val_{726}, Ala_{743} and Lys_{745}) (Fig. 3).

Table 2
Analysis of the interaction between breast cancer target and synthesized molecules.

Ligands	Docking energies (Kcal/mol)	Ligands	Docking energies (Kcal/mol)
3a	−6.0	3 g	−7.4
3b	−6.1	3 h	−6.7
3c	−5.5	3i	−6.9
3d	−6.7	3 j	−6.9
3e	−7.0	3k	−5.3
3f	−7.1	7	−7.7

4. Results and discussions

Among all the synthesized compounds, **3b** and **3h** shows potent anticancer activity against breast cancer cell line. MCF-7 and MDA-MB-231 but their activities were more pronounced in aggressive breast cancer model (MDA-MB-231 cells) with IC_{50} 13μM and 5μM respectively. Out of the series **compound 3h** was the most active and potent analogue with lowest IC_{50} against MDA-MB-231 cells. Interestingly, **compound 3h** shows no cytotoxicity against HEK-293 cells suggesting that **compound 3h** was probably the safest compound of this series with specific activity against cancer cells.

Compound 3h arrest progression of cells at G0/G1 check point

Compound 3h dose dependently inhibited progression of cell cycle at G0/G1 check point (Fig. 4). Furthermore, dose dependent increase of sub-diploid populations were also increased which indicate possible DNA fragmentation and apoptosis of MDA-MB-231 cells due to **compound 3h** treatment.

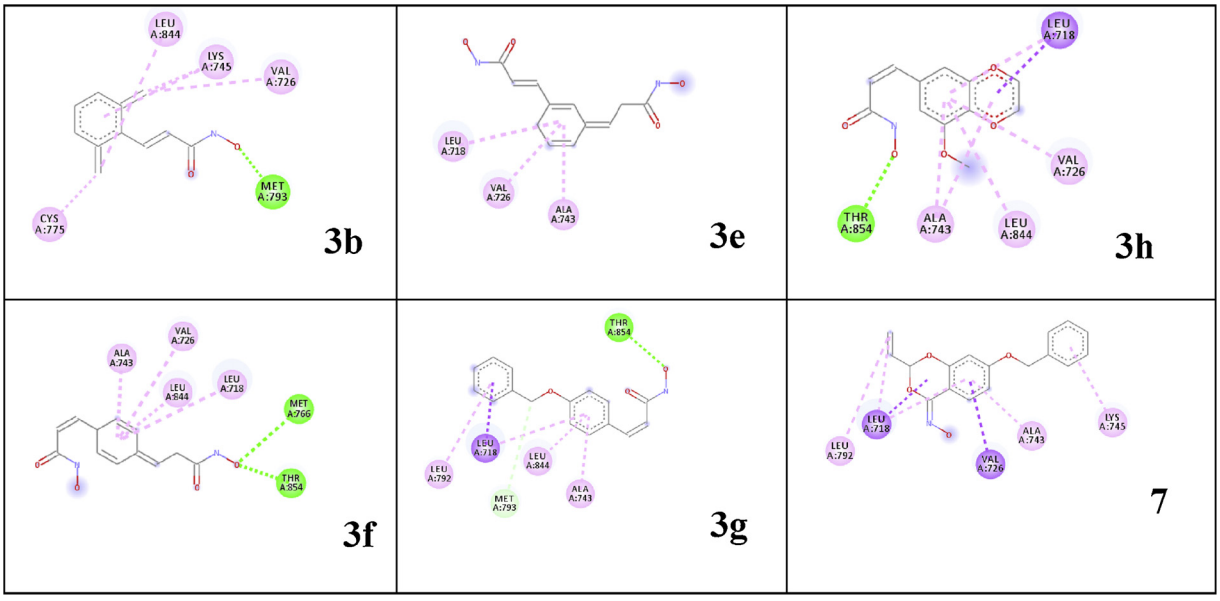

Fig. 2. Interaction between EGFR target and 3b, 3e–3h and 7.

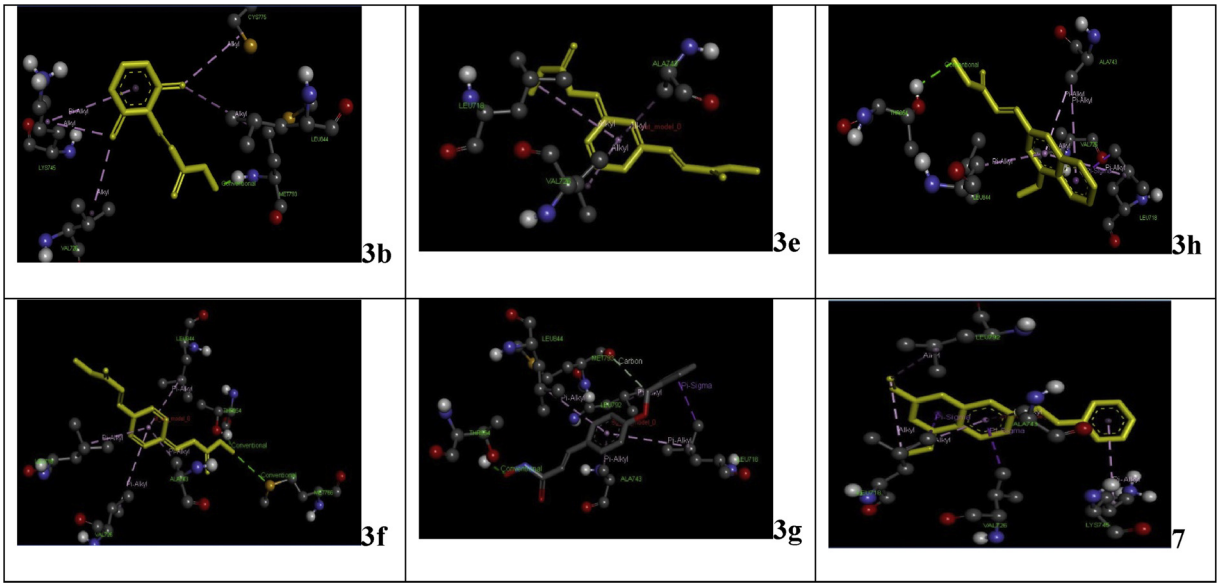

Fig. 3. 3D Structure of docking image of 3b, 3e–3h and 7 with EGFR target protein.

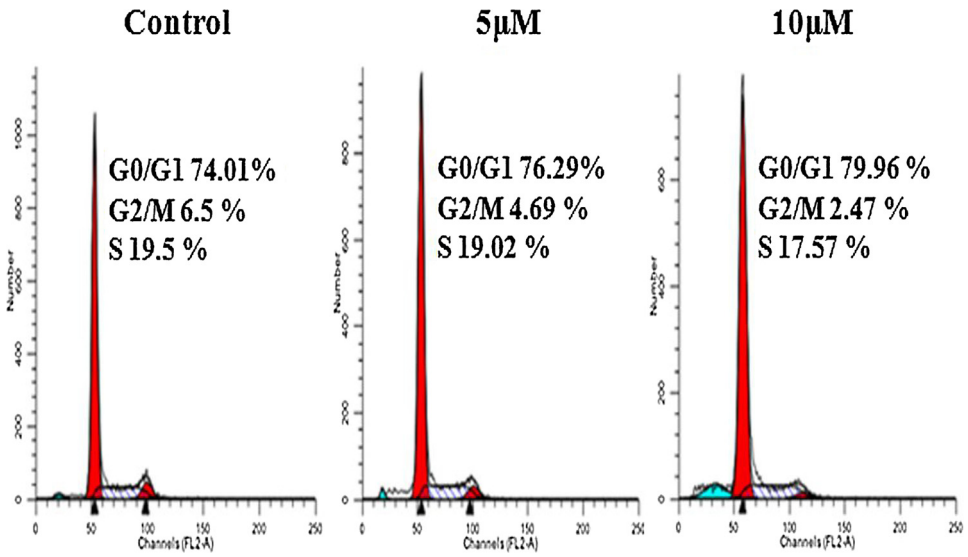

Fig. 4. Effect of **compound 3h** on cell cycle progression in MDA-MB-231 cells. Cells were treated with **compound 3h** for 24 h washed with PBS, stained with PI and analyzed by flow cytometry. Quantification of flow cytometry data has been shown as percent of total cells.

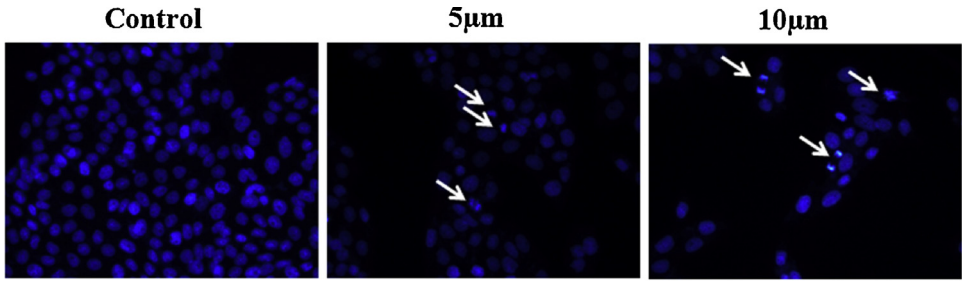

Fig. 5. Effect of **compound 3h** on nuclear morphology in MDA-MB-231 cells. Cells were treated with **compound 3h** for 24 h washed with PBS, fixed with paraformaldehyde, stained with Hoechst-33358 and analyzed by fluorescent microscopy.

Compound 3h induces DNA damage and apoptosis in MDA-MB-231 cells

If any compound treatment causes DNA damage and fragmentation, altered nuclear morphology of MDA-MB-231 cells can be monitored with DNA binding fluorescent Hoechst stain under florescence microscopy. In this case, **compound 3h** induced dose-dependent DNA fragmentations in treated group as compared to non-treated vehicle control clearly indicating cells were undergoing apoptosis due to compound exposure (Fig. 5). This data was further confirmed by flow cytometry using Annexin V-FITC/PI dual staining technique. Results

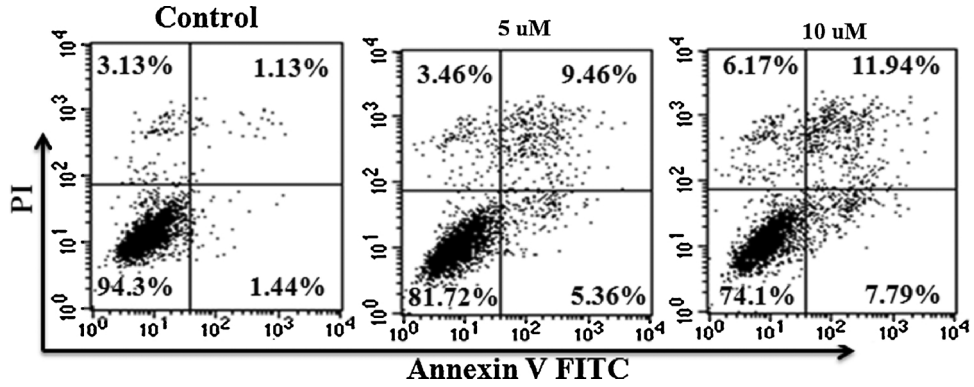

Fig. 6. Effect of **compound 3h** on apoptosis in MDA-MB-231 cells. Cells were treated with **compound 3h** for 24 h washed with PBS, stained with Annexin V-FITC/PI and analyzed by flow cytometry. Quantification of flow cytometry data has been shown as percent of total cells.

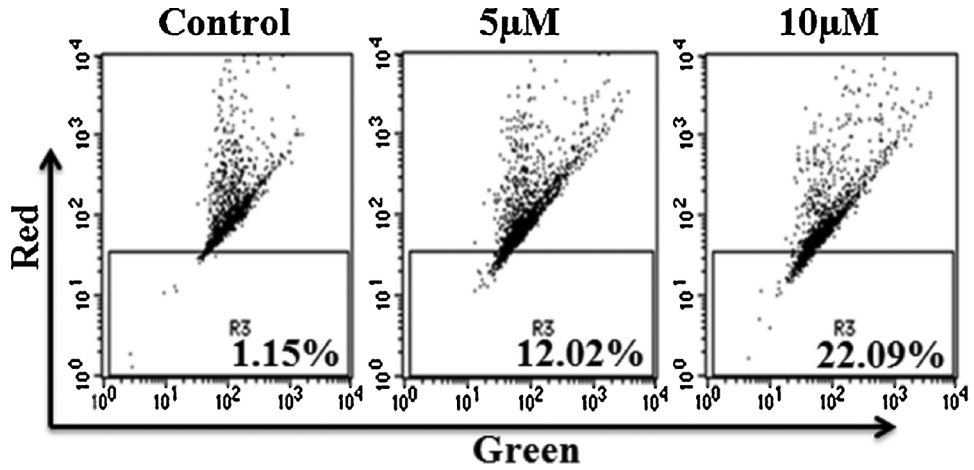

Fig. 7. Effect of **compound 3h** on MMP in MDA-MB-231 cells. Cells were treated with **compound 3h** for 24 h, washed with PBS, stained with JC-1 and analyzed by flow cytometry. Quantification of flow cytometry data has been shown as percent of total cells.

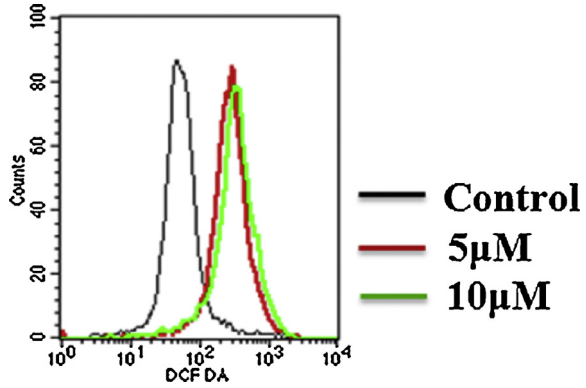

Fig. 8. Effect of **compound 3h** on ROS generation in MDA-MB-231 cells. Cells were treated with **compound 3h** for 24 h washed with PBS, stained with DCFH-DA and analyzed by flow cytometry.

showed that **compound 3h** induces apoptosis dose dependently in MDA-MB-231 cells as compared to non-treated vehicle control cells (Fig. 6).

Compound 3h induce MMP loss in MDA-MB-231 cells

Further, effect of **compound 3h** on mitochondria as alterations in MMP was carried out using membrane potential sensitive dye JC-1. Any increase in intensity of green fluorescence from red fluorescence of JC-1 dye stained cells indicates mitochondrial depolarization. Flow cytometric data indicate increase of green fluorescence in MDA-MB-231 cells with treatment of increasing concentration of **compound 3h** (Fig. 7). This clearly indicates significant loss of MMP in MDA-MB-231 cells due to **compound 3h** treatment.

Compound 3h induce ROS generation in MDA-MB-231 cells

Reactive oxygen species (ROS) is a well-known mediator of apoptosis and majority of chemotherapeutics detrimental to cancer cells due to their ROS inducing capacity [48,49]. As **compound 3h** induces apoptosis, it is possible that it might induce ROS in MDA-MB-231 cells. Therefore, effect of **compound 3h** on ROS generation in MDA-MB-231 cells was evaluated by flow cytometry using DCFH-DA dye. Flow cytometric data revealed that treatment of **compound 3h** significantly induced ROS generation compared to non-treated vehicle control MDA-MB-231 cells (Fig. 8).

5. Conclusions

The present study investigates the anticancer effects of *N*-Hydroxycinnamamide derivatives in human breast cancer cells. Molecular docking results showed that **3b, 3e–3h** and **7** could act on the active sites of pro-apoptotic proteins EGFR to induce apoptotic death of cancer cells. Out of twelve compounds screened, **compound 3b** and **compound 3h** exhibits most potent activity against aggressive breast cancer cells (MDA-MB-231) with IC_{50} 13 μM and 5 μM respectively. **Compound 3h** inhibits cell cycle progression by accumulating cells at G0/G1 check points. Moreover, **compound 3h** promotes DNA fragmentation and induction of apoptosis. Furthermore, loss of mitochondrial membrane were also potentially induced by **compound 3h**. One of the major mechanisms of action of **compound 3h** for its anticancer activity is probably induction of ROS in cancer cells thereby

inducing apoptotic cell deaths in cancer cells. Our findings suggest that **compounds3b** and **3h** might be considered as potential candidates for novel anticancer drug in the future.

Conflicts of interest

The authors have declared that there are no conflicts of interest.

Acknowledgement

The authors thank the UGC fellowship for financial support of this research work.

Appendix A. Supplementary data

Supplementary material related to this article can be found, in the online version, at doi:https://doi.org/10.1016/j.biopha.2018.08.015.

References

[1] A. Hematpoor, M. Paydar, S.Y. Liew, Y. Sivasothy, N. Mohebali, C.Y. Looi, et al., Phenylpropanoids isolated from Piper sarmentosum Roxb. induce apoptosis in breast cancer cells through reactive oxygen species and mitochondrial-dependent pathways, Chem. Biol. Interact. 279 (2018) 210–218.
[2] M. Dahlui, S. Ramli, A.M. Bulgiba, Breast cancer prevention and control programs in Malaysia, Asian Pac. J. Cancer Prev. 12 (2011) 1631–1634.
[3] B. Bachmeier, I. Fichtner, P.H. Killian, E. Kronski, U. Pfeffer, T. Efferth, Development of resistance towards artesunate in MDA-MB-231 human breast cancer cells, PLoS One 6 (2011) e20550.
[4] K.J. Chavez, S.V. Garimella, S. Lipkowitz, Triple negative breast cancer cell lines: one tool in the search for better treatment of triple negative breast cancer, Breast Dis. 32 (2010) 35.
[5] N.D. Kokare, D.B. Shinde, N-[(Diphenoxyphosphoryl) oxy]-2-phenyl-1H-benzimidazole as a versatile reagent for synthesis O-alkylhydroxamic acids, J. Heterocycl. Chem. 45 (2008) 981–986.
[6] P. Marks, Discovery and development of SAHA as an anticancer agent, Oncogene 26 (2007) 1351.
[7] B. Kumar, A. Yadav, J.C. Lang, T.N. Teknos, P. Kumar, Suberoylanilide hydroxamic acid (SAHA) reverses chemoresistance in head and neck cancer cells by targeting cancer stem cells via the downregulation of nanog, Genes Cancer 6 (2015) 169.
[8] F. Foss, R. Advani, M. Duvic, K.B. Hymes, T. Intragumtornchai, A. Lekhakula, et al., A Phase II trial of Belinostat (PXD101) in patients with relapsed or refractory peripheral or cutaneous T-cell lymphoma, Br. J. Haematol. 168 (2015) 811–819.
[9] P. Atadja, Development of the pan-DAC inhibitor panobinostat (LBH589): successes and challenges, Cancer Lett. 280 (2009) 233–241.
[10] Y. Song, T. Hai, Y. Wang, R. Guo, W. Li, L. Wang, et al., Epigenetic reprogramming, gene expression and in vitro development of porcine SCNT embryos are significantly improved by a histone deacetylase inhibitor—m-carboxycinnamic acid bishydroxamide (CBHA), Protein Cell 5 (2014) 382–393.
[11] B. Eigl, S. North, E. Winquist, D. Finch, L. Wood, S. Sridhar, et al., A phase II study of the HDAC inhibitor SB939 in patients with castration resistant prostate cancer: NCIC clinical trials group study IND195, Invest. New Drugs 33 (2015) 969–976.
[12] A.T. Brunetto, J.E. Ang, R. Lal, D. Olmos, L.R. Molife, R. Kristeleit, et al., First-in-human, pharmacokinetic and pharmacodynamic phase I study of Resminostat, an oral histone deacetylase inhibitor, in patients with advanced solid tumors, Clin. Cancer Res. 19 (2013) 5494–5504.
[13] M. Paris, M. Porcelloni, M. Binaschi, D. Fattori, Histone deacetylase inhibitors: from bench to clinic, J. Med. Chem. 51 (2008) 1505–1529.
[14] G. Zhao, H. Zhong, X. Qiu, S. Wang, Y. Gao, Z. Dai, et al., The DFT study of cyclohexyl hydroxamic acid as a collector in scheelite flotation, Miner. Eng. 49 (2013) 54–60.
[15] M. Varasi, F. Thaler, A. Abate, C. Bigogno, R. Boggio, G. Carenzi, et al., Discovery, synthesis, and pharmacological evaluation of spiropiperidine hydroxamic acid based derivatives as structurally novel histone deacetylase (HDAC) inhibitors, J. Med. Chem. 54 (2011) 3051–3064.
[16] A. Thorarensen, M.R. Douglas Jr., D.C. Rohrer, A.F. Vosters, A.W. Yem, V.D. Marshall, et al., Identification of novel potent hydroxamic acid inhibitors of peptidyl deformylase and the importance of the hydroxamic acid functionality on inhibition, Bioorg. Med. Chem. Lett. 11 (2001) 1355–1358.
[17] M.R. Gowravaram, J.S. Johnson, D. Delecki, E.R. Cook, B.E. Tomczuk, A.K. Ghose, et al., Inhibition of matrix metalloproteinases by hydroxamates containing heteroatom-based modifications of the P1'group, J. Med. Chem. 38 (1995) 2570–2581.
[18] A. Scozzafava, C.T. Supuran, Carbonic anhydrase and matrix metalloproteinase inhibitors: sulfonylated amino acid hydroxamates with MMP inhibitory properties act as efficient inhibitors of CA isozymes I, II, and IV, and N-hydroxysulfonamides inhibit both these zinc enzymes, J. Med. Chem. 43 (2000) 3677–3687.
[19] N.L. Tsakadze, S.D. Sithu, U. Sen, W.R. English, G. Murphy, S.E. D'Souza, Tumor necrosis factor-α-converting enzyme (TACE/ADAM-17) mediates the ectodomain cleavage of intercellular adhesion molecule-1 (ICAM-1), J. Biol. Chem. 281 (2006) 3157–3164.
[20] L. Lum, B.R. Wong, R. Josien, J.D. Becherer, H. Erdjument-Bromage, J. Schlöndorff, et al., Evidence for a role of a tumor necrosis factor-α (TNF-α)-converting enzyme-like protease in shedding of TRANCE, a TNF family member involved in osteoclastogenesis and dendritic cell survival, J. Biol. Chem. 274 (1999) 13613–13618.
[21] J.E. Bolden, M.J. Peart, R.W. Johnstone, Anticancer activities of histone deacetylase inhibitors, Nat. Rev. Drug Discov. 5 (2006) 769.
[22] C. Salmi-Smail, A. Fabre, F. Dequiedt, A. Restouin, R. Castellano, S. Garbit, et al., Modified cap group suberoylanilide hydroxamic acid histone deacetylase inhibitor derivatives reveal improved selective antileukemic activity, J. Med. Chem. 53 (2010) 3038–3047.
[23] M.B. Plewe, S.L. Butler, K.R. Dress, Q. Hu, T.W. Johnson, J.E. Kuehler, et al., Azaindole hydroxamic acids are potent HIV-1 integrase inhibitors, J. Med. Chem. 52 (2009) 7211–7219.
[24] S. Bertrand, J.-J. Hélesbeux, G. Larcher, O. Duval, Hydroxamate, a key pharmacophore exhibiting a wide range of biological activities, Mini Rev. Med. Chem. 13 (2013) 1311–1326.
[25] J. Levin, M. Du, Sulfonate ester hydroxamic acids as potent and selective inhibitors of TACE enzyme, Drug Des. Discov. 18 (2003) 123–126.
[26] E. Nuti, F. Casalini, S.I. Avramova, S. Santamaria, G. Cercignani, L. Marinelli, et al., NO-isopropyl sulfonamido-based hydroxamates: design, synthesis and biological evaluation of selective matrix metalloproteinase-13 inhibitors as potential therapeutic agents for osteoarthritis, J. Med. Chem. 52 (2009) 4757–4773.
[27] A.T. Shaw, D.-W. Kim, R. Mehra, D.S. Tan, E. Felip, L.Q. Chow, et al., Ceritinib in ALK-rearranged non–small-cell lung cancer, N. Engl. J. Med. 370 (2014) 1189–1197.
[28] L. Chen, R. Petrelli, G. Gao, D.J. Wilson, G.T. McLean, H.N. Jayaram, et al., Dual inhibitors of inosine monophosphate dehydrogenase and histone deacetylase based on a cinnamic hydroxamic acid core structure, Bioorg. Med. Chem. 18 (2010) 5950–5964.
[29] Y. Nagaoka, T. Maeda, Y. Kawai, D. Nakashima, T. Oikawa, K. Shimoke, et al., Synthesis and cancer antiproliferative activity of new histone deacetylase inhibitors: hydrophilic hydroxamates and 2-aminobenzamide-containing derivatives, Eur. J. Med. Chem. 41 (2006) 697–708.
[30] S. Chopra, E.D. Beaulieu, J.P. Malerich, Natural products as anti-infective agents, Front. Anti-Infect. Drug Discov. 2 (2014) 159.
[31] Y. Komatsu, K.-y. Tomizaki, M. Tsukamoto, T. Kato, N. Nishino, S. Sato, et al., Cyclic hydroxamic-acid-containing peptide 31, a potent synthetic histone deacetylase inhibitor with antitumor activity, Cancer Res. 61 (2001) 4459–4466.
[32] J.E. Jackman, C.A. Fierke, L.N. Tumey, M. Pirrung, T. Uchiyama, S.H. Tahir, et al., Antibacterial agents that target lipid a biosynthesis in gram-negative bacteria inhibition of diverse UDP-3-O-(R-3-hydroxymyristoyl)-N-acetylglucosamine deacetylases by substrate analogs containing zinc binding motifs, J. Biol. Chem. 275 (2000) 11002–11009.
[33] A.S. Reddy, M.S. Kumar, G.R. Reddy, A convenient method for the preparation of hydroxamic acids, Tetrahedron Lett. 41 (2000) 6285–6288.
[34] Y.-J. Park, T.-J. Kim, Y.-H. Cho, Y.-J. Jung, H.-J. Im, K.-S. Song, et al., EPR investigation on a quantitative analysis of Eu (II) and Eu (III) in LiCl/KCl eutectic molten salt, Bull. Korean Chem. Soc. 29 (2008) 127–129.
[35] C.J. Marmion, T. Murphy, J.R. Docherty, K.B. Nolan, Hydroxamic acids are nitric oxide donors. Facile formation of ruthenium (II)-nitrosyls and NO-mediated activation of guanylate cyclase by hydroxamic acids, Chem. Commun. (2000) 1153–1154.
[36] P. Loll, C. Sharkey, S. O'Connor, C. Dooley, E. O'Brien, M. Devocelle, et al., O-acetylsalicylhydroxamic acid, a novel acetylating inhibitor of prostaglandin H2 synthase: structural and functional characterization of enzyme-inhibitor interactions, Mol. Pharmacol. 60 (2001) 1407–1413.
[37] C. Dooley, M. Devocelle, B. McLoughlin, K. Nolan, D. Fitzgerald, C. Sharkey, A novel family of hydroxamate-based acylating inhibitors of cyclooxygenase, Mol. Pharmacol. 63 (2003) 450–455.
[38] P. Bali, M. Pranpat, R. Swaby, W. Fiskus, H. Yamaguchi, M. Balasis, et al., Activity of suberoylanilide hydroxamic acid against human breast cancer cells with amplification of her-2, Clin. Cancer Res. 11 (2005) 6382–6389.
[39] D.M. Floyd, A.W. Fritz, J. Pluscec, E.R. Weaver, C.M. Cimarusti, Monobactams, Preparation of (S)-3-amino-2-oxoazetidine-1-sulfonic acids from L-. alpha.-amino-. beta.-hydroxy acids via their hydroxamic esters, J. Org. Chem. 47 (1982) 5160–5167.
[40] R.M. Williams, B.H. Lee, Synthesis of a 1, 3-bridged. beta.-lactam: a novel, anti-Bredt. beta.-lactam, J. Am. Chem. Soc. 108 (1986) 6431–6433.
[41] K. Nagarajan, S. Rajappa, P. Rajagopalan, P. Talwalkar, Hydroxamic acid derivatives with potential antiinflammatory activity, Indian J. Chem. Sect. B: Org. Chem. Incl. Med. Chem. 30 (1991) 222–229.
[42] J.A. Panza, A.A. Quyyumi, J.E. Brush Jr., S.E. Epstein, Abnormal endothelium-dependent vascular relaxation in patients with essential hypertension, N. Engl. J. Med. 323 (1990) 22–27.
[43] A. Krüger, M.J. Arlt, M. Gerg, C. Kopitz, M.M. Bernardo, M. Chang, et al., Antimetastatic activity of a novel mechanism-based gelatinase inhibitor, Cancer Res. 65 (2005) 3523–3526.
[44] M.J. Miller, Syntheses and therapeutic potential of hydroxamic acid based siderophores and analogs, Chem. Rev. 89 (1989) 1563–1579.
[45] E. Slesak, M. Slesak, B. Gabrys, Effect of methyl jasmonate on hydroxamic acid content, protease activity, and bird cherry–oat aphid Rhopalosiphum padi (L.) probing behavior, J. Chem. Ecol. 27 (2001) 2529–2543.
[46] T. Kanji, A. Mitsuo, S. Reiji S. Substituted benzohydroxamates. Google Patents; 1967.
[47] V. Kukshal, M. Mishra, A. Ajay, T. Khanam, R. Sharma, D. Dube, et al., Synthesis and bioevaluation of aryl hydroxamates distinguishing between NAD+ and ATP-dependent DNA ligases, MedChemComm 3 (2012) 453–461.
[48] H.-U. Simon, A. Haj-Yehia, F. Levi-Schaffer, Role of reactive oxygen species (ROS) in apoptosis induction, Apoptosis 5 (2000) 415–418.
[49] N. Devender, K. Ramakrishna, S.K. Shukla, R. Konwar, R.P. Tripathi, Synthesis and anticancer activity of γ-(triazolyl ethylidene) butenolides and polyfunctional pyrrolinones, Eur. J. Med. Chem. 82 (2014) 106–119.